

Nickel(II) Complex of 6,6'-Bis(hexylbenzoylamino)-2,2'-bipyridine as a Functional Carrier: pH-Induced Affinity-Switching and Mechanism of the SCN⁻-Selective Up-Hill Transport

Sung-Kil Lee, Yoshinori Kumasaka, Joe Otsuki, and Koji Araki*

Institute of Industrial Science, The University of Tokyo, 7-22-1 Roppongi, Minato-ku, Tokyo 106

(Received November 7, 1995)

The Ni(II) complex of 6,6'-bis(hexylbenzoylamino)-2,2'-bipyridine (LH₂) in square-planar symmetry underwent a reversible and simultaneous deprotonation of the two amide units. The non-deprotonated complex (NiLH₂²⁺) showed high SCN⁻ selectivity by the preferential axial coordination of two SCN⁻ molecules ($\log K_{\text{SCN}} = 8.11 \pm 0.03$ in CH₂Cl₂ at 20 °C), while the deprotonated complex showed little affinity toward anions. Deprotonation-induced affinity-switching of the complex by the external aqueous layer mediated an efficient SCN⁻-selective up-hill transport across a CH₂Cl₂ liquid membrane by coupling with the symport of protons from pH 4.0 to 6.0 aqueous solutions. Equilibrium at the aqueous/organic interface could be represented by the equation $K_{\text{app}} = ([\text{Ni}(\text{LH}_2)(\text{SCN})_2]_{\text{org}})/([\text{NiL}]_{\text{org}}[\text{H}^+]_{\text{aq}}^2[\text{SCN}^-]_{\text{aq}}^2)$, where K_{app} is the equilibrium constant ($\log K_{\text{app}} = 13.6$ at 20 °C). However, the rates of protonation and deprotonation of the complex at the interface were dependent mostly on the concentration of the complex in the organic layer. Based on these results, detailed mechanisms of the transport are discussed.

The selective and active transport of substrates across cell membranes is one of the essential functions of biological membranes.¹⁾ As a model of membrane transport in living systems, carrier-mediated transport across an artificial membrane has been extensively investigated.^{2–5)} Since the substrate affinity of the carrier must be high in the uptake process, but low in the release process, in order to achieve highly efficient transport,⁶⁾ we have been studying functional carriers whose affinity can be switched in the transport process by photoirradiation or a pH difference.^{7,8)}

In a previous paper,⁹⁾ we reported that the Cu(II) complex of 6,6'-bis(hexylbenzoylamino)-2,2'-bipyridine (LH₂) serves as an efficient and selective carrier in the pH-driven up-hill transport of anions. The complex in organic solvents undergoes reversible deprotonation of the amide groups by contact with external aqueous solutions (Scheme 1). The deprotonated complex has no affinity toward anions, while the complex in the non-deprotonated form shows high affinity toward lipophilic anions. The extraction of lipophilic anions by the non-deprotonated complex and deprotonation-induced switching of the affinity at the other membrane interface mediated an efficient up-hill transport of anions by coupling with the proton concentration gradient across the membrane. In the case of SCN⁻, having a high coordination ability, preferential axial coordination of SCN⁻ to the metal center in square-planar symmetry made the transport highly SCN⁻-selective. However, deprotonation of the Cu(II) complex proceeded stepwise from the mono-deprotonated to the fully-deprotonated form (Scheme 1 (i)). Furthermore, axial coordination of SCN⁻ to the metal center of the non-depro-

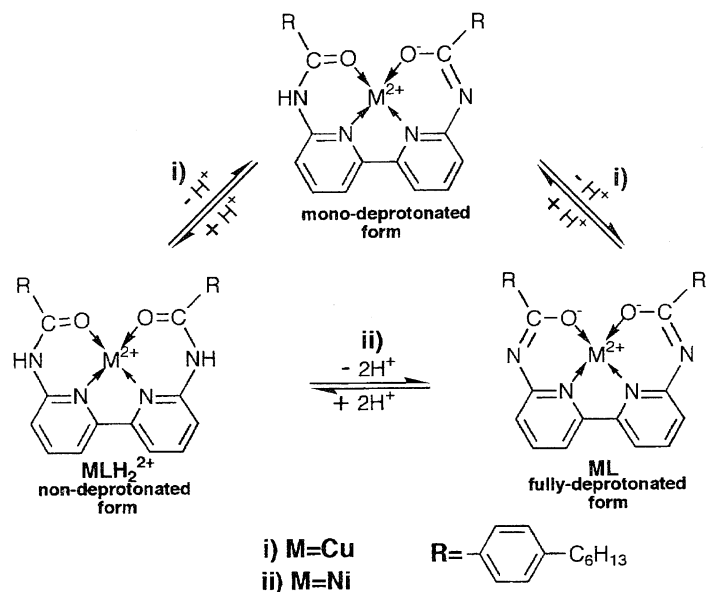
tonated complex also took place stepwise from the mono- to bis-coordinated species. These complicated equilibrium did not allow us to determine the stoichiometry of the anions bound to the carrier complex, and no further analysis of the transport mechanism could be carried out. In this study we used the Ni(II) complex of LH₂ as the carrier, which showed a much simpler stoichiometry and a slightly better performance compared to that of the Cu(II) complex in the SCN⁻-selective up-hill transport. Thus, we quantitatively examined the pH-induced affinity switching of the complex, and clarified the mechanism of transport mediated by the functional Ni(II) complex.

Experimental

Measurements: Thermal analyses were carried out using a Mettler FP90 thermo system and a Rigaku Thermo Plus TG-DTA system. The FTIR spectra were recorded on a Perkin-Elmer 1600 series FTIR spectrometer. The electronic spectra were measured using a Shimadzu UV 2200 or a Photol MCPD 1000 spectrophotometer at 20 °C.

Quantitative analyses of anions were carried out by the following methods: SCN⁻ by a colorimetric method according to the standard procedure, Br⁻ using an anion-selective electrode (Br-125, Toa Electronics Ltd., Tokyo), and *p*-toluenesulfonate (*p*-tol) by absorbance at 261 nm.

Materials: The solvents and other chemicals were obtained commercially, and were purified by routine methods, if necessary. 6,6'-Bis(hexylbenzoylamino)-2,2'-bipyridine (LH₂) was prepared from 6,6'-diamino-2,2'-bipyridine and 4-hexylbenzoyl chloride according to a reported procedure.¹⁰⁾ The preparation of the Ni(II) complex was essentially the same as that of the Cu(II) complex.⁹⁾



Scheme 1. Deprotonation of the complex.

[Ni(LH₂)(H₂O)₂](NO₃)₂(H₂O)₂ (NiLH₂²⁺): Pale green plates (yield 65%, ca. 80 °C (−H₂O by TG), 100–112 °C (−H₂O by TG), 124–133 °C (−H₂O by TG), and 192–203 °C (−2HNO₃ by TG, decomp); IR (KBr) 3324, 1644, 1617, 1539, 1385, and 1317 cm^{−1}. Found: C, 52.71; H, 5.71; N, 10.50%. Calcd for C₃₆H₅₀N₆NiO₁₂: C, 52.89; H, 6.16; N, 10.28; Ni, 7.18%.

[Ni(h-babp)] (NiL): Orange needles (yield 97%), mp 177.3–178.6 °C; IR (KBr) 1494, 1417, and 1381 cm^{−1}. Found: C, 69.64; H, 6.11; N, 8.97%. Calcd for C₃₆H₄₀N₄NiO₂: C, 69.81; H, 6.51; N, 9.04; Ni, 9.48%.

Equilibrium Studies in Two-Phase Systems: The following aqueous and organic solutions (3 cm³ for each) were placed together in a 20-cm³ capped cylindrical bottle; after 60 min of mixing by a Yamato shaker model MD-21 (200 rpm), the bottle was left to stand for 30 min and the aqueous and organic layers were analyzed separately: aqueous layer, a Kolthoff's buffer solution (mixtures of 0.05 mol dm^{−3} sodium succinate and 0.05 mol dm^{−3} sodium tetraborate, pH 3.0–6.0) containing an appropriate concentration of sodium salts; the organic layer, a dichloromethane solution containing Ni(LH₂)(NO₃)₂.

Kinetic Studies in Two-Phase Systems: Uptake Process: To an organic NiL solution (3.3–10.0 × 10^{−5} mol dm^{−3}, 2 cm³, CH₂Cl₂+5% CH₃OH) in a quartz-made UV cell of a 1 × 1 × 6.4 (height)-cm size at 20 °C, a Kolthoff's buffer solution (2 cm³, pH 3.4–4.0) containing NaSCN (1.0–20.0 × 10^{−3} mol dm^{−3}) was quickly, but carefully, placed in order to minimize any effect of the initial contact of the two solutions. Rough contact of the two solutions resulted in an immediate conversion of NiL to Ni(LH₂)(SCN)₂. The organic layer was stirred at 480 rpm by an Iuchi Multi Stirrer M-3. The conversion of NiL to Ni(LH₂)(SCN)₂ was monitored by a Photol MCPD 1000 spectrophotometer at 20 °C.

Release Process: A non-deprotonated complex, Ni(LH₂)(SCN)₂, was prepared quantitatively by mixing a Ni(LH₂)(NO₃)₂/(CH₂Cl₂+5% CH₃OH) solution (3.2–7.7 × 10^{−5} mol dm^{−3}) with an aqueous NaSCN solution (pH 4.0, 0.3–10.0 × 10^{−2} mol dm^{−3}). The resultant Ni(LH₂)(SCN)₂ solution was used as the organic layer. The procedure for monitoring the conversion of Ni(LH₂)(SCN)₂ to NiL after contact with aqueous buffer solutions (pH 6.0–6.6) was essentially the same as that for

the uptake process.

Transport Experiments in Three-Phase Systems: Transport experiments were carried out at 20 °C according to a previously reported procedure.⁹ The organic layer (30 cm³, CH₂Cl₂+5% CH₃OH) was placed at the bottom of a cylindrical glass cell (diameter 4 cm, height 6 cm), and the two aqueous layers (10 cm³ for each) set on the organic layer were separated from each other by a glass plate inserted at the center of the cell. During the transport experiment, the organic layer was slowly stirred with a small magnetic stirrer so as to allow the interface of the aqueous and organic layers to swirl slowly (ca. 80 rpm).

Results

Properties of the Ni(II) Complexes: The Ni(II) complex of 6,6'-bis(benzoylamino)-2,2'-bipyridine has previously been shown to have an N₂O₂-type square-planar structure.¹⁰ In this study, hexyl groups were introduced to the benzoyl units of this parent compound in order to increase the lipophilicity of the complex. The IR and electronic spectra of the Ni(II) complex with LH₂ were essentially the same as those of the Ni(II) complex of the parent compound.¹⁰ Therefore, the introduction of hexyl groups did not affect the N₂O₂ square-planar structure of the complex.

Spectral titration of NiLH₂²⁺ in dichloromethane by methanolic NaOH showed a clear one-step spectral change with isosbestic points at 330 and 358 nm (Fig. 1). The addition of more than two molar amounts of NaOH did not cause any further spectral change, and the spectra became identical to that of the fully-deprotonated complex NiL. Therefore, a simultaneous deprotonation of the two amide units directly converted the non-deprotonated complex to the fully-deprotonated form, in contrast to the corresponding Cu(II) complex, which underwent stepwise deprotonation through the mono-deprotonated form (Scheme 1).⁹ Amide deprotonation of the complex was confirmed to be reversible by the repeated addition of methanolic HCl and NaOH.

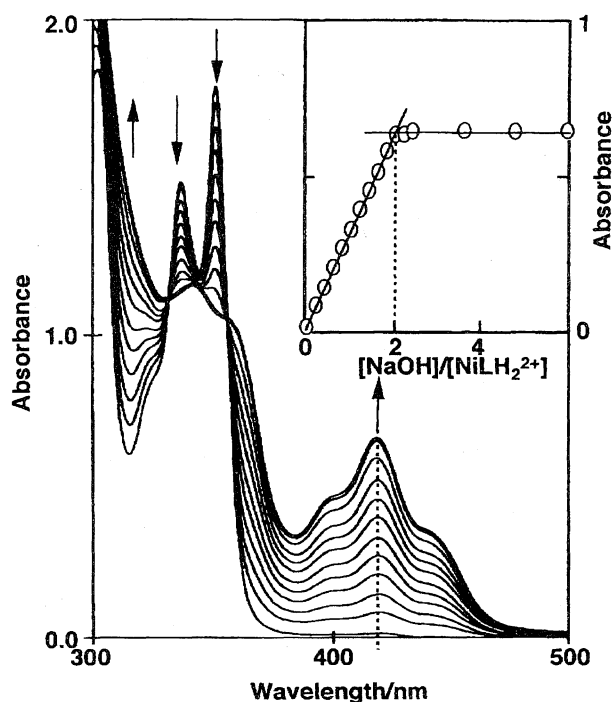


Fig. 1. Spectral change of $\text{Ni}(\text{LH}_2)(\text{NO}_3)_2$ ($8.12 \times 10^{-5} \text{ mol dm}^{-3}$) in CH_2Cl_2 (containing 5% CH_3OH) upon addition of small amounts of methanolic NaOH, where $[\text{NaOH}]/[\text{Complex}]$ molar ratios were 0 to 6. Absorbances at 421 nm were shown as an inset.

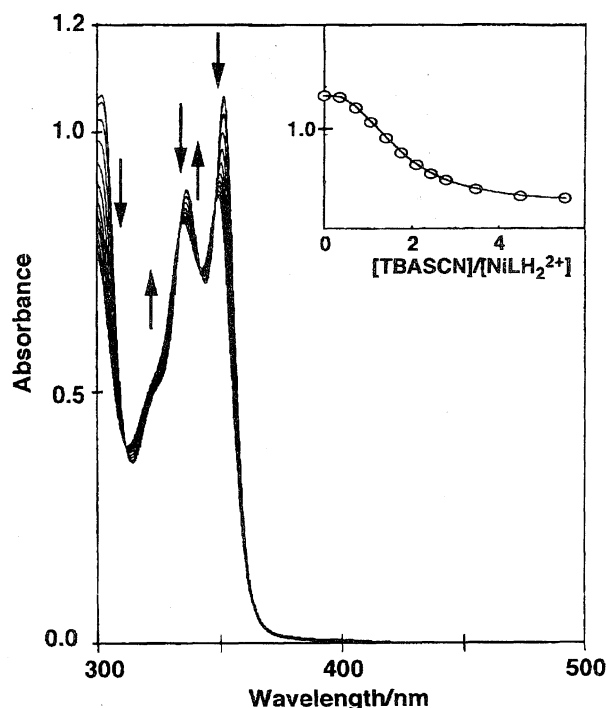


Fig. 2. Spectral change of $\text{Ni}(\text{LH}_2)(\text{NO}_3)_2$ ($4.82 \times 10^{-5} \text{ mol dm}^{-3}$) in CH_2Cl_2 (containing 5% CH_3OH) upon addition of (TBA)SCN at 20°C , where $[(\text{TBA})\text{SCN}]/[\text{Complex}]$ molar ratios were 0 to 5.53. Absorbances at 351.6 nm were shown as an inset together with the simulated curve.

Anion Affinity of the Transition Metal Complexes:

The electronic spectrum of the deprotonated complex NiL in dichloromethane at 20°C was little affected by the presence of tetra-*n*-butylammonium (TBA) bromide, *p*-toluenesulfonate (*p*-tol), and thiocyanate. The ligand-centered π - π^* band of the non-deprotonated complex $\text{Ni}(\text{LH}_2)(\text{NO}_3)_2$ in dichloromethane showed a small, but clear, blue-shift in a one-step on addition of (TBA)SCN up to nearly two-times the molar amounts (Fig. 2), though TBA salts of bromide and *p*-tol showed no effect on the spectra. In the case of CuLH_2^{2+} , a similar, but stepwise, spectral change was observed due to the stepwise coordination of two SCN^- from the axial position.⁹⁾ Therefore, the observed spectral change for the Ni(II) complex is also ascribed to the axial coordination of two SCN^- to the metal center. No spectral change was observed for bromide and *p*-tol, having weak coordination ability, indicating that they did not interact directly with the complex. Based on Scheme 2, the association constant for SCN^- (K_{SCN}) was determined from the absorbance at 351.6 nm by a curve fitting method. From the satisfactory curve fitting (shown as an inset of Fig. 2), $\log K_{\text{SCN}}$ was determined to be 8.11 ± 0.03 ($r^2 = 0.996$), which shows a high SCN^- affinity of the non-deprotonated complex. Since a fully-deprotonated complex having stronger square-planar ligand field showed no sign of interaction, even with SCN^- ,

the deprotonation of the complex caused a drastic change in the SCN^- -affinity. Similar, but not quantitative, results were obtained for the Cu(II) complex.⁹⁾ However, the Ni(II) complex is markedly different concerning its equilibria in amide deprotonation and SCN^- coordination. The simple one-step equilibria of the Ni(II) complex are advantageous in analyzing the transport mechanism.

Equilibrium Studies in the Two-Phase System: The solute equilibrium between aqueous and organic layers was studied in the two-phase system. For these studies, equilibrium between the aqueous buffer and the dichloromethane layer was established by vigorous mixing of the two solutions for 60 min. No leakage of the complex from the organic layer was observed at all. Figure 3 shows the pH profiles of the molar fraction of the deprotonated complex in the organic layer. The results confirmed that the deprotonation of the complex in the organic layer was controlled by the pH, type of anion, and anion concentration of the aqueous buffer solution. Hydrophilic bromide in the aqueous layer hardly affected the complex in the organic layer, while lipophilic, but weak, coordinating anions, such as *p*-tol and perchlorate, increased the molar fraction of the non-deprotonated form moderately. However, the presence of SCN^- , having a high affinity toward the non-deprotonated complex, showed



Scheme 2.

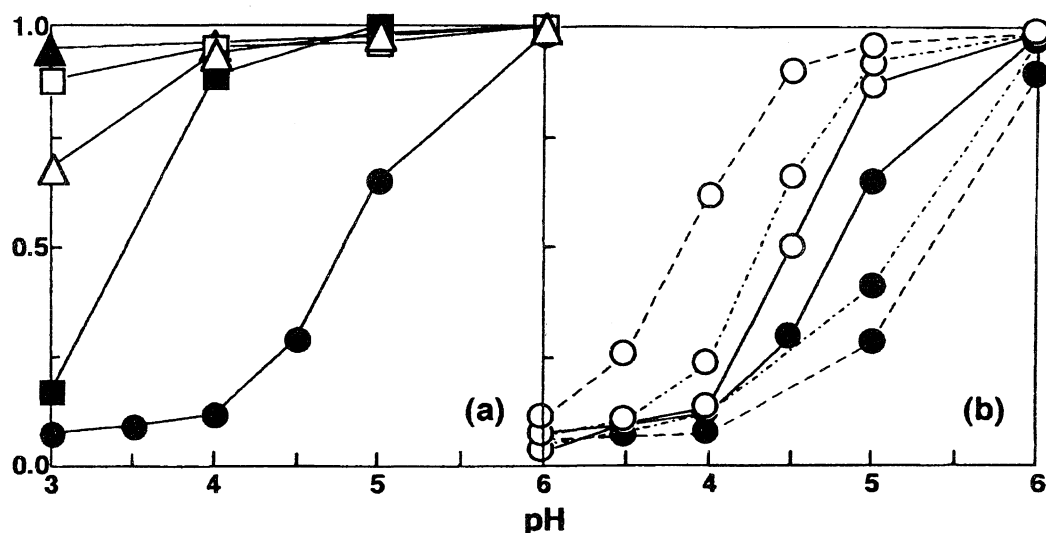


Fig. 3. pH profiles of the molar fraction of NiL in the organic layer after mixing with aqueous buffer solutions containing different (a) type of sodium salts and (b) NaSCN concentrations. (a) Type of sodium salts ($1.0 \times 10^{-2} \text{ mol dm}^{-3}$); —▲—: no salt, —●—: NaSCN, —■—: Na *p*-tol, —△—: NaClO₄ and —□—: NaBr. (b) NaSCN concentrations; ---○---: 1.0×10^{-3} , --○--: 3.0×10^{-3} , —○—: 5.0×10^{-3} , —●—: 1.0×10^{-2} , -.-●-.-: 2.0×10^{-2} , and ---●---: $4.0 \times 10^{-2} \text{ mol dm}^{-3}$.

a drastic change in the composition, and a higher concentration of SCN^- greatly increased the non-deprotonated form. Figure 4 shows the amounts of SCN^- transferred into the organic layer after contact with aqueous solutions. By increasing the SCN^- concentration in the aqueous layer at pH 4.0, the $\text{SCN}^-/\text{complex}$ molar ratio in the organic layer approached close to two. Therefore, two molar amounts of SCN^- were transferred into the organic layer by the non-deprotonated complex, which is in good agreement with the previous observation of bis- SCN^- coordination to the non-deprotonated complex. From a pH 6.0 aqueous solution, a negligible amount of SCN^- was transferred into the organic layer. Since contact with the aqueous pH 6.0 solution made the complex to be in the fully-deprotonated form, the results confirmed that the deprotonated complex has no ability to extract SCN^- from an aqueous solution.

Transport of Anions by pH-Induced Affinity-Switching

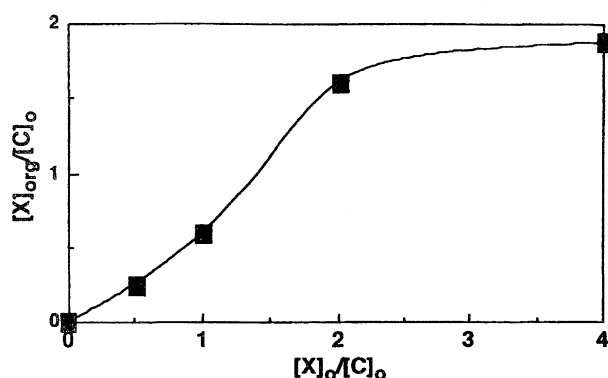


Fig. 4. Effect of the initial SCN^- concentration ($[X]_o$) in the aqueous buffer solution (pH 4.0) on the concentration of the extracted SCN^- ($[X]_{org}$) in the organic layer. Initial NiLH_2^{2+} concentration ($[C]_o$) in CH_2Cl_2 was $2.0 \times 10^{-3} \text{ mol dm}^{-3}$. See experimental section for detailed conditions.

of the Ni(II) Complex Carrier: Transport experiments were carried out at 20°C according to a previously reported procedure.⁹⁾ Although two aqueous buffer layers, I and II (aq I and II), were identical in their volume (10 cm^3) and initial SCN^- concentration ($1.00 \times 10^{-2} \text{ mol dm}^{-3}$), their pH values were different (aq I: 3.0—5.0, and aq II: 6.0). The two aqueous layers were separated by the organic layer (dichloromethane with 5 v/v% methanol, 30 cm^3) containing NiLH_2^{2+} ($1.11 \times 10^{-4} \text{ mol dm}^{-3}$). When the pH of aq I was 4.0 or 3.0 (Fig. 5), the efficient up-hill transport of SCN^- was mediated from aq I to the aq II. No SCN^- transport was observed without the Ni(II) complex, confirming that the complex serves as the carrier. The initial stage of transport from aq I (pH 4.0) to aq II (pH 6.0) is summarized in Table 1. The pH increase in aq I and the decrease in aq II indicated that the up-hill transport of SCN^- was coupled with the symport of protons across the membrane.

Although lipophilic *p*-tol was also transported across the organic layer, hydrophilic bromide was not transported at all (Table 2). When *p*-tol and SCN^- were present simultaneously in the aqueous layers, SCN^- was selectively transported, showing that the coordination ability is the critical factor concerning the transport selectivity.

Kinetic Analysis of Up-Hill Transport: To understand the efficient up-hill transport of SCN^- by the Ni(II) complex, kinetic studies of the SCN^- -transfer between the organic and aqueous layers were carried out. When the aqueous buffer solution at pH 4.0 containing NaSCN was carefully layered on the organic NiL solution, a rapid conversion of NiL to $\text{Ni}(\text{LH}_2)(\text{SCN})_2$ in the organic layer was observed by the spectrophotometric method. This indicates an efficient transfer of protons and SCN^- from the aqueous to the organic solutions. The effect of the initial contact of the two solutions diminished within 0.5 min, and the rate of conversion of NiL to $\text{Ni}(\text{LH}_2)(\text{SCN})_2$ (v) followed first-order kinetics

Table 1. Initial Stage of the SCN^- Transport from the Aqueous Layers I (10 cm^3 , pH 4.0) to II (10 cm^3 , pH 6.0) across the CH_2Cl_2 Layer Containing NiLH_2^{2+} ($0.97 \times 10^{-4} \text{ mol dm}^{-3}$, 30 cm^3) at 20°C

Time h	Aq I (pH 4.0)		Aq II (pH 6.0)		Organic layer
	$[\text{SCN}^-]$	pH	$[\text{SCN}^-]$	pH	$[\text{NiLH}_2^{2+}]$
	$\times 10^{-2} \text{ mol dm}^{-3}$		$\times 10^{-2} \text{ mol dm}^{-3}$		molar fraction
0	1.00	4.00	1.00	6.00	0.95
3	0.86	4.08	1.01	5.95	0.60
12	0.58	4.17	1.22	5.75	0.57
24	0.41	4.24	1.52	5.60	0.55

Table 2. Anion Transport from the Aqueous Layers I (10 cm^3) to II (10 cm^3 , pH 6.0) across the CH_2Cl_2 Layer Containing NiLH_2^{2+} ($1.11 \times 10^{-4} \text{ mol dm}^{-3}$, 30 cm^3) at $20^\circ\text{C}^{\text{a}}$

No.	Anion	Initial pH of Aq I	Anion concentration after 72 h		Turn-over ^{c)}
			10 ⁻² mol dm ⁻³		
			Aq I	Aq II	
1	SCN ⁻	3.0	0.12	1.82	12.3
2	SCN ⁻	4.0	0.24	1.59	8.9
3	Br ⁻	4.0	1.00	1.00	0.0
4	<i>p</i> -Tol	4.0	0.84	1.04	0.6
5 ^{b)}	<i>p</i> -Tol	3.0	0.99	1.00	0.0
6 ^{b)}	SCN ⁻		0.15	1.85	12.8
	<i>p</i> -Tol	4.0	0.82	1.04	0.6
	SCN ⁻		0.29	1.43	8.0

a) Initial anion concentrations in the aqueous layers I and II were $1.00 \times 10^{-2} \text{ mol dm}^{-3}$. b) The aqueous layers contained both *p*-tol and SCN^- . c) Turn-over of the carrier after 72 h was calculated from the amounts of anions transported to aq II based on the assumption that twice molar amount of substrates is transported by the carrier.

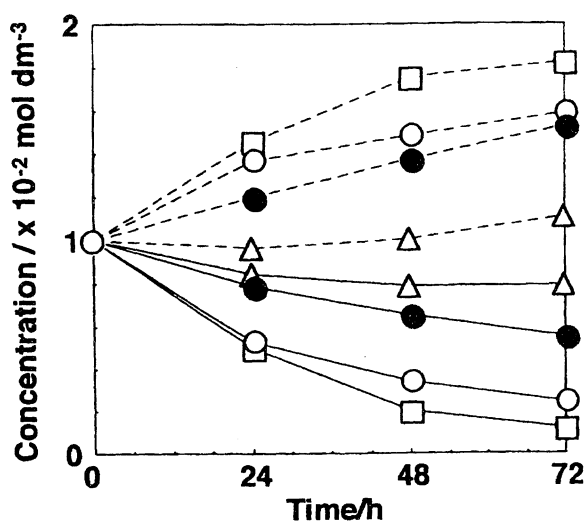


Fig. 5. Time course of the SCN^- concentrations of the aqueous layers I (—) and II (---) during the SCN^- transport by NiLH_2^{2+} ($1.11 \times 10^{-4} \text{ mol dm}^{-3}$) in the three-phase system at 20°C . Initial concentrations of SCN^- in both aqueous layers were $1 \times 10^{-2} \text{ mol dm}^{-3}$. The layer II was set at pH 6.0, while pH of the layer I was 3.0 (\square), 4.0 (\circ), and 5.0 (\triangle). For comparison, the SCN^- transport by CuLH_2^{2+} from the pH 4.0 aqueous layer I under similar conditions (\bullet) was also shown in the figure.

(Fig. 6(a)). The initial rates of conversion (v°) in mol min^{-1} are shown in Fig. 7 as functions of the NiL concentration in the organic solution, NaSCN concentration, and pH of the aqueous solution.

The SCN^- transfer from the organic to aqueous solutions was studied similarly. Again, the rate of conversion of $\text{Ni}(\text{LH}_2)(\text{SCN})_2$ to NiL followed first-order kinetics (Fig. 6(b)); the effects of the solute concentrations on the initial rates are shown in Fig. 8.

Discussion

pH-Induced Affinity-Switching of the Ni(II) Complex Carrier and Their Performance in Anion Transport:

The results shown in Fig. 5 demonstrate that the Ni(II) complex of LH_2 mediated the efficient and selective up-hill transport of anions by coupling with the pH difference across the liquid membrane. Although the deprotonated complex has no affinity toward anions, the non-deprotonated complex shows a moderate-to-high affinity toward the lipophilic anions, and an especially high affinity toward SCN^- , having a high coordination ability. Anions were incorporated in and transported across the organic membrane by the non-deprotonated form of the complex; affinity switching of the carrier by reversible deprotonation allows efficient up-hill transport by coupling with the proton symport.

The binding of anions with the non-deprotonated complex is primarily due to an electrostatic interaction; lipophilic

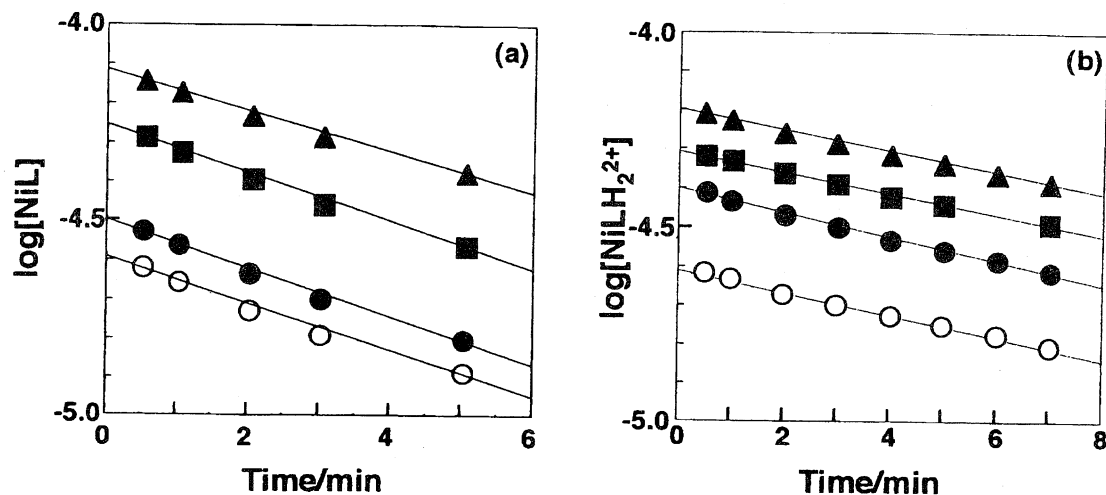


Fig. 6. Time course of concentration of (a) the deprotonated complex in the uptake process and (b) the non-deprotonated complex in the release process.

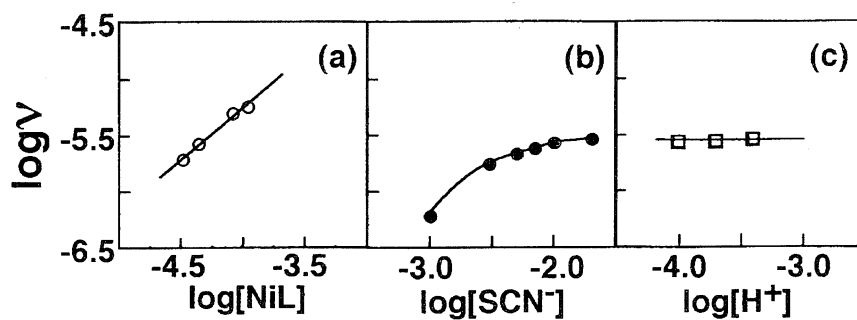


Fig. 7. Rate of conversion (v) of NiL to $\text{Ni}(\text{LH}_2)(\text{SCN})_2$ at 20 °C as functions of a) NiL concentration in the organic, b) NaSCN concentration in the aqueous, and c) pH of the aqueous solutions. Parameters other than specified were set at following standard conditions; NiL: $4.40 \times 10^{-5} \text{ mol dm}^{-3}$, NaSCN: $1.0 \times 10^{-2} \text{ mol dm}^{-3}$, and pH 4.0.

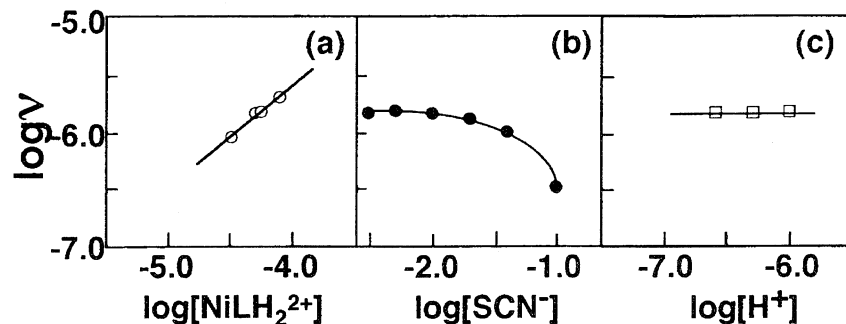


Fig. 8. Rate of conversion (v) of $\text{Ni}(\text{LH}_2)(\text{SCN})_2$ to NiL at 20 °C as functions of a) $\text{Ni}(\text{LH}_2)(\text{SCN})_2$ concentration in the organic, b) NaSCN concentration in the aqueous, and c) pH of the aqueous solutions. Parameters other than specified were set at following standard conditions; NiLH_2^{2+} : $4.91 \times 10^{-5} \text{ mol dm}^{-3}$, NaSCN: $1.0 \times 10^{-2} \text{ mol dm}^{-3}$, and pH 6.0.

counter anions are favorable in organic media. In the case of SCN^- , however, the spectral change indicated the axial coordination of two SCN^- molecules to the metal center (Fig. 2); the association of SCN^- to the complex was almost quantitative ($\log K_{\text{SCN}} = 8.11 \pm 0.03$), showing a high SCN^- affinity. Therefore, the high transport selectivity of the Ni(II) complex carrier toward SCN^- is ascribed to the high coordination ability of SCN^- at the uptake process.

These results are essentially the same as those observed for the Cu(II) complex.⁹⁾ However, the SCN^- transport was too

complicated to study in detail when the Cu(II) complex was used as the carrier. Both the non-deprotonated and mono-deprotonated complexes were the potential carrier in the organic layer because of the stepwise deprotonation of the Cu(II) complex; furthermore, the number of SCN^- incorporated by the non-deprotonated complex could not be determined due to the stepwise coordination of SCN^- . On the other hand, the Ni(II) complex exists either in the non-deprotonated or fully-deprotonated form, but not in the mono-deprotonated form, and the coordination of two SCN^- molecules

to the non-deprotonated complex takes place simultaneously. Therefore, SCN^- is incorporated into the organic layer only as $\text{Ni}(\text{LH}_2)(\text{SCN})_2$. This simple stoichiometry allows us to analyze the SCN^- transport in further detail.

Equilibrium at the Membrane Interface: In aqueous/organic two-phase equilibrium experiments, no leakage of the complex into the aqueous layer was observed. Therefore, the apparent solute equilibrium in the system can be represented as Scheme 3, where K_{app} is the equilibrium constant, and is given as

$$K_{\text{app}} = \frac{[\text{Ni}(\text{LH}_2)(\text{SCN})_2]_{\text{org}}}{[\text{SCN}^-]_{\text{aq}}^2 [\text{H}^+]_{\text{aq}} [\text{NiL}]_{\text{org}}}, \quad (1)$$

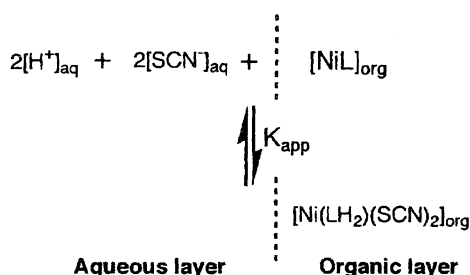
or

$$\log K_{\text{app}} = 2\text{pH} - 2\log [\text{SCN}^-]_{\text{aq}} + \log ([\text{Ni}(\text{LH}_2)(\text{SCN})_2]_{\text{org}} / [\text{NiL}]_{\text{org}}),$$

where suffix $_{\text{aq}}$ or $_{\text{org}}$ indicates the aqueous or organic layer, respectively. Here, we defined $\text{pH}_{1/2}$ as the pH of the aqueous layer at which the molar fraction $[\text{Ni}(\text{LH}_2)(\text{SCN})_2]_{\text{org}} / [\text{NiL}]_{\text{org}}$ becomes unity at given $[\text{SCN}^-]_{\text{aq}}$ concentrations. Equation 1 can be transformed into

$$\text{pH}_{1/2} = 1/2 \log K_{\text{app}} + \log [\text{SCN}^-]_{\text{aq}}, \quad (2)$$

The $\text{pH}_{1/2}$ values obtained from Fig. 3(b) were plotted as a function of $\log [\text{SCN}^-]$ (Fig. 9). The observed good linear correlation assures the validity of the solute equilibrium in



Scheme 3.

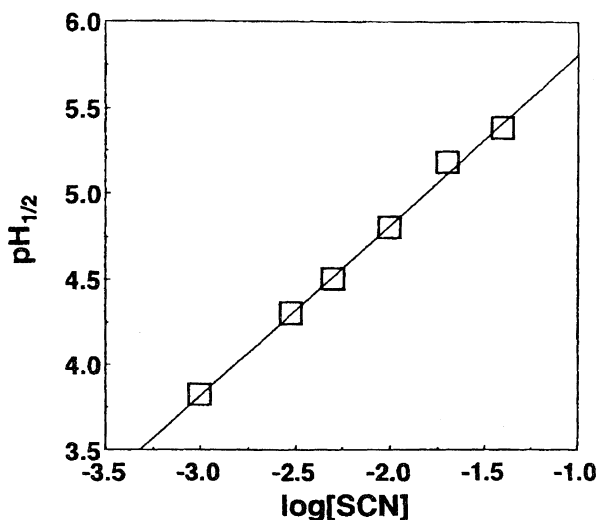


Fig. 9. Plot of $\text{pH}_{1/2}$ vs. $\log [\text{SCN}^-]$ according to the Eq. 2.

the system (Scheme 3), and $\log K_{\text{app}}$ was determined to be 13.6 from the intersection. A lower pH or a higher SCN^- concentration of the aqueous layer increases the molar fraction of the non-deprotonated complex, confirming that the reversible deprotonation of the complex in the organic membrane can be controlled by the external aqueous layer.

To change the $[\text{Ni}(\text{LH}_2)(\text{SCN})_2]_{\text{org}} / [\text{NiL}]_{\text{org}}$ ratio from 0.1 to 10 by the pH of the external aqueous solution, the pH difference of one is estimated to be sufficient from the Eq. 1. The simultaneous protonation of the two amide units of the deprotonated complex results in a second-order dependence of the equilibrium on the proton concentration, which makes the deprotonation curve steeper. Figure 3 confirms that a small pH difference is indeed sufficient to control the deprotonation equilibrium of the complex; therefore, switching its anion affinity by a small pH difference realizes an efficient up-hill transport of SCN^- .

Kinetics of Solute Transfer at the Aqueous/Organic Interface: In the uptake process, the conversion of NiL to $\text{Ni}(\text{LH}_2)(\text{SCN})_2$ followed first-order kinetics after the initial mixing effect was completed. As shown in Fig. 7, the rate ν° is linearly dependent on the initial NiL concentration in the organic layer. However, the effect of the SCN^- concentration in the aqueous layer becomes evident only when the SCN^- concentration is sufficiently low. The rate does not depend on the proton concentration in the aqueous layer. The conversion of NiL to $\text{Ni}(\text{LH}_2)(\text{SCN})_2$ involves the simultaneous transfer of two molar amounts of SCN^- and H^+ across the aqueous/organic interface; the rate of conversion (ν°) corresponds to half the rates of the SCN^- and H^+ transfer in $\text{mol min}^{-1} \text{cm}^{-2}$ from the aqueous to the organic layers (surface area = 1 cm^2). Since the rate of conversion depends linearly on the NiL concentration in the organic layer, but not much on the SCN^- and H^+ concentrations in the aqueous layer, the rate-determining step in the uptake process may be the diffusion of NiL to the interface where association with SCN^- and H^+ takes place. Since no leakage of the complex to the aqueous layer was observed at all, the results suggest that the association of the complex takes place at the interface more closer to the aqueous phase.

In the release process, similar results were obtained. Again, the rate of conversion from $\text{Ni}(\text{LH}_2)(\text{SCN})_2$ to NiL is mostly dependent on the initial $\text{Ni}(\text{LH}_2)(\text{SCN})_2$ concentration, not on the initial SCN^- or proton concentration in the aqueous layer, though a sufficiently high SCN^- concentration moderately decreased the rate.

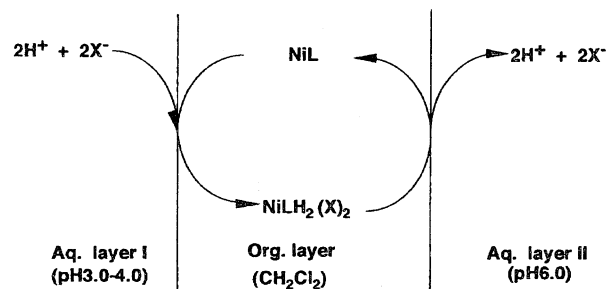
The moderate dependence on the SCN^- concentration (Figs. 7 and 8) can be explained from the shift of the $[\text{Ni}(\text{LH}_2)(\text{SCN})_2] / [\text{NiL}]$ equilibrium in the organic layer from Eq. 1. The lowest SCN^- concentration studied here was $1.0 \times 10^{-3} \text{ mol dm}^{-3}$ in the uptake process (pH 4.0); highest in the release process was $1.0 \times 10^{-1} \text{ mol dm}^{-3}$ (pH 6.0). When the solute equilibrium was attained, $\log ([\text{Ni}(\text{LH}_2)(\text{SCN})_2] / [\text{NiL}])$ was estimated to be -0.4 for both cases from the $\log K_{\text{app}}$ value of 13.6 (Eq. 1). This estimation indicates that the molar fraction of $\text{Ni}(\text{LH}_2)(\text{SCN})_2$ in the uptake process is only 0.3 at the lowest SCN^- concentration, even after

attaining equilibrium, or that of NiL in the release process is shifted to 0.7 at the highest SCN^- concentration. Therefore, the observed decrease of the rates in Fig. 7 at a lower SCN^- concentration, and Fig. 8 at a higher SCN^- concentration, can be attributed to a shift in the equilibrium.

Kinetics of the Transport by the Ni(II) Complex: As shown in Table 1, more than half of the SCN^- in aq I had been transferred from aq I (pH 4.0) by the Ni(II) complex carrier within 24 h. During 3 to 12 h of transport, the molar fraction of $\text{Ni}(\text{LH}_2)(\text{SCN})_2$ in the organic membrane changed only from 0.60 to 0.57. Therefore, the transport system is regarded to be in a steady state; the average of these values represents the molar fraction of $\text{Ni}(\text{LH}_2)(\text{SCN})_2$ during this period. Based on the assumption that the rate is dependent only of the NiL concentration in the organic layer under the experimental conditions, the rate of the SCN^- transfer at the uptake process was estimated to be $1.0 \times 10^{-8} \text{ mol min}^{-1} \text{ cm}^{-2}$ from the rate of conversion of NiL to $\text{Ni}(\text{LH}_2)(\text{SCN})_2$, shown in Fig. 7(a).¹¹⁾ Similarly, the rate of SCN^- release at the organic/aq II interface was estimated to be $7.0 \times 10^{-9} \text{ mol min}^{-1} \text{ cm}^{-2}$ from Fig. 8(a).¹¹⁾ Thus, the amounts of SCN^- transferred across the aq I/organic membrane and the organic membrane/aq II interfaces (each interface area is 6.28 cm^2) during transport between 3 and 12 h were estimated to be 3.4×10^{-5} and $2.4 \times 10^{-5} \text{ mol}$, respectively. The values estimated from the two-phase experiment agree with those obtained from the transport experiment in the three-phase system. Since the volume of the aqueous layers is 10 cm^3 , the amounts of the SCN^- transferred from aq I and to aq II during this time period were determined experimentally to be 2.8×10^{-5} and $2.1 \times 10^{-5} \text{ mol}$, respectively, from Table 1. Therefore, the interfacial process which we observed in the two-phase system was indeed operating similarly in the three-phase system.

The pH of aq I and aq II during transport from 3 to 12 h shifted from 4.08 and 5.95 to 4.17 and 5.75, respectively (Table 1). Titration of the buffer solutions with a concd HCl or NaOH solution indicated that the observed pH shifts required $2.2 \times 10^{-5} \text{ mol}$ of proton decrease in aq I and $2.6 \times 10^{-5} \text{ mol}$ of increase in aq II. The results coincided roughly with the observed amount of the transported SCN^- . Therefore, the up-hill transport of SCN^- is coupled quantitatively with the proton symport. A quantitative coupling of SCN^- transport with the proton transport is realized by the simultaneous binding of protons and SCN^- to the NiL to form $\text{Ni}(\text{LH}_2)(\text{SCN})_2$, which mediates an efficient pH-driven up-hill transport.

In summary, we demonstrated that the affinity switching of the Ni(II) complex of LH_2 induces an efficient up-hill transport of SCN^- by coupling with the pH difference. The simple one-step amide-deprotonation and SCN^- coordination permitted a quantitative analysis of the transport mechanism illustrated in Scheme 4. The following are the major features of this transport system: high SCN^- affinity of the non-deprotonated complex in the organic layer ($\log K_{\text{SCN}} = 8.11 \pm 0.03$); high SCN^- extractability of the non-deprotonated complex from the aqueous layer ($\log K_{\text{app}} = 13.6$); a small



Scheme 4.

pH difference of the external aqueous solution required for regulating the deprotonation-induced affinity switching of the carrier, and quantitative coupling with the proton symport.

In the case of a biological membrane system, an ATP-driven ion pump across a membrane is often described using an 'alternate access' model.¹²⁻¹⁴⁾ In this model, the position of the binding site is assumed to remain unchanged as the binding cavity opens alternatively to the uptake and discharge sides of the membrane, and switching of the ion-binding affinity mediates the efficient active transport of ions. The results presented here demonstrated that the affinity-switching strategy is also effective to mediate efficient up-hill transport in a carrier-mediated transport system.

Part of this study is supported by a Grant-in-Aid for Scientific Research No. 0723028 from the Ministry of Education, Science and Culture.

References

- 1) A. Kotyk, K. Janacek, and J. Koryta, "Biophysical Chemistry of Membrane Functions," John Wiley & Sons, Chichester (1988).
- 2) R. Hilgenfeld, R. M. Kellogg, D. Landini, F. Montanari, G. R. Painter, B. C. Pressman, F. Rolla, and W. Saenger, "Host Guest Complex Chemistry II," ed by F. Vögtle, Springer-Verlag, Berlin (1982).
- 3) J. S. Schultz, "Synthetic Membranes: Science, Engineering and Applications," ed by P. M. Bungay, H. K. Lonsdale, and M. N. de Pinho, D. Reidel Publishing Co., Dordrecht (1986), pp. 523-566.
- 4) J.-M. Lehn, "Supramolecular Chemistry: Concepts and Perspectives," ed by C. St. Cooper, VCH, Weinheim (1995), pp. 69-80.
- 5) K. Maruyama, H. Tsukube, and T. Araki, *J. Am. Chem. Soc.*, **104**, 5197 (1982).
- 6) M. Seno, and K. Araki, "New Functionality Materials," ed by T. Tsuruta, M. Seno, and M. Doyama, Elsevier Science Publishers, Amsterdam (1993), Vol. C, pp. 465-472.
- 7) M. Ino, J. Otsuki, K. Araki, and M. Seno, *J. Membr. Sci.*, **89**, 101 (1994).
- 8) M. Ino, H. Tanaka, J. Otsuki, K. Araki, and M. Seno, *Colloid Polym. Sci.*, **272**, 151 (1994).
- 9) K. Araki, S.-K. Lee, and J. Otsuki, *J. Chem. Soc., Dalton Trans.*, in press.
- 10) M. Yamada, K. Araki, and S. Shiraishi, *Bull. Chem. Soc. Jpn.*, **61**, 2767 (1988).

11) Rate of the conversion of NiL at the NiL concentration of $4.0 \times 10^{-5} \text{ mol dm}^{-3}$ was $2.5 \times 10^{-6} \text{ mol dm}^{-3} \text{ min}^{-1}$, or $5.0 \times 10^{-9} \text{ mol min}^{-1}$ (volume of the organic layer was 2 cm^3) from the two-phase experiment (Fig. 7(a)). Since the interface area of the two-phase system was 1 cm^2 , rate of the SCN^- -transfer was $1.0 \times 10^{-8} \text{ mol min}^{-1} \text{ cm}^{-2}$. Similarly, rate of the conversion of

$\text{Ni}(\text{LH}_2)(\text{SCN})_2$ at the concentration of $5.7 \times 10^{-5} \text{ mol dm}^{-3}$ was $1.7 \times 10^{-6} \text{ mol dm}^{-3} \text{ min}^{-1}$ or $3.5 \times 10^{-9} \text{ mol min}^{-1}$, and rate of the SCN^- -transfer was $7.0 \times 10^{-9} \text{ mol min}^{-1} \text{ cm}^{-2}$.

12) C. Tanford, *Annu. Rev. Biochem.*, **45**, 379 (1983).

13) C. Tanford, *Proc. Natl. Acad. Sci. U.S.A.*, **79**, 2882 (1982).

14) M. H. Hao and S. C. Harvey, *Biochim. Biophys. Acta*, **5**, 1234 (1995).
